

New Mechanism for the Ring-Opening Polymerization of Lactones? Uranyl Aryloxy-Induced Intermolecular Catalysis

Aurora Walshe,[†] Jian Fang,^{‡,§} Laurent Maron,^{*,‡} and Robert J. Baker^{*,†}

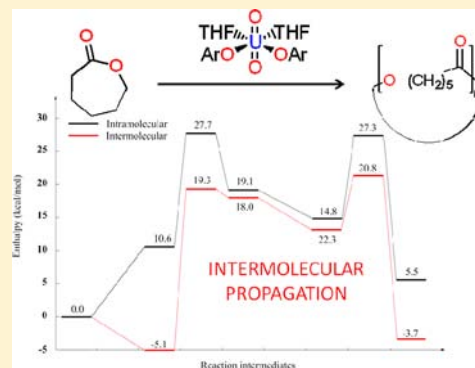
[†]School of Chemistry, University of Dublin, Trinity College, Dublin 2, Ireland

[‡]LPCNO, INSA Toulouse, 137 Avenue de Rangueil, 31077 Toulouse, France

[§]College of Chemistry and Chemical Engineering, Lanzhou University, Lanzhou 730000, China

Supporting Information

ABSTRACT: The uranyl aryloxy $[\text{UO}_2(\text{OAr})_2(\text{THF})_2]$ ($\text{Ar} = 2,6\text{-}^t\text{Bu}_2\text{-C}_6\text{H}_2$) is an active catalyst for the ring-opening *cyclo*-oligomerization of ϵ -caprolactone and δ -valerolactone but not for β -butyrolactone, γ -butyrolactone, and *rac*-lactide. ^1H EXSY measurements give the thermodynamic parameters for exchange of monomer and coordinated THF, and rates of polymerization have been determined. A comprehensive theoretical examination of the mechanism is discussed. From both experiment and theory, the initiation step is intramolecular and in keeping with the accepted mechanism, while computational studies indicate that propagation can go via an intermolecular pathway, which is the first time this has been observed. The lack of polymerization for the inactive monomers has been investigated theoretically and C–H $\cdots\pi$ interactions stabilize the coordination of the less rigid monomers.

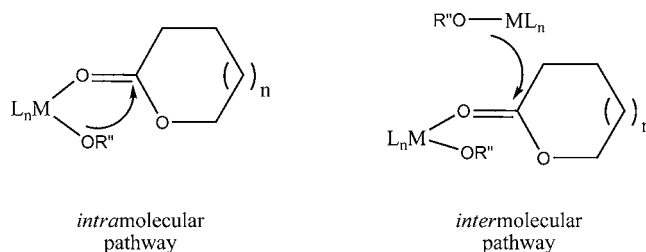


INTRODUCTION

The coordination and organometallic chemistry of uranium has undergone a renaissance of interest over the past few years and great advances have been reported for U(III) compounds, where results in small molecule activation is nothing short of outstanding.¹ New reactivity patterns are being uncovered that have no parallel with d-block or lanthanide metal compounds.² In contrast, the chemistry of the uranyl ion has not been explored to such an extent, but a study of the nonaqueous chemistry of $[\text{UO}_2]^{2+}$ have produced results that challenge our ideas of structure and bonding in this ion.³ Recent highlights include the isolation of a uranyl⁴ and uranium(VI) carbene,⁵ reduction to uranyl(V)⁶ and the synthesis of SMM incorporating a $[\text{UO}_2]^+$ moiety,⁷ supramolecular uranyl peroxides that show distinct topologies⁸ and the use of uranyl compounds in the catalysis of monomers that contain oxygen.⁹ We have reported on the latter, where uranyl aryloxy $[\text{UO}_2(\text{OAr})_2(\text{THF})_2]$ (**1**; $\text{Ar} = 2,6\text{-}^t\text{Bu}_2\text{-C}_6\text{H}_2$) or uranyl chloride $[\text{UO}_2\text{Cl}_2(\text{THF})_3]$ can act as an effective catalyst for the ring-opening polymerization of epoxides. This is unusual in that the commonly held belief was that oxygen-containing monomers were incompatible with oxophilic actinide ions. Lin and Marks' early study demonstrated a marked decrease in rate of hydrogenolysis of the metal bound alkyl group in $[\text{Cp}^*\text{Th}(\text{R})(\text{OR})]$ relative to that in $[\text{Cp}^*\text{ThR}_2]$,¹⁰ and this myth has only recently been challenged by Eisen and co-workers.¹¹ We have carried out a comprehensive computational study on this reaction and concluded that for uranyl chloride an intermolecular mechanism for initiation and propagation was favored and that coordination of the monomer to the uranyl

ion also polarized the C–O bonds.¹² However, due to the increase in steric bulk in the uranyl aryloxy, the mechanism was *intramolecular* in initiation and *intermolecular* in propagation, that is, the monomer is coordinated to one metal and a second metal delivers the nucleophile during propagation (Scheme 1).

Scheme 1. Inter and Intramolecular Ring-Opening Pathways for the Ring-Opening Polymerization of Cyclic Lactones



We therefore reasoned that the uranyl ion may engender different reactivity toward the ring-opening polymerization of lactones whereby the accepted mechanism for a coordination–insertion type is exclusively *cis*-migratory insertion (intramolecular).¹³ There are a number of examples where homo- and heterobimetallic compounds act as precatalysts but these proceed *via* the *cis*-migratory insertion mechanism by way of dissociation of a ligand to form mononuclear species,¹⁴ or

Received: May 21, 2013

Published: July 23, 2013

where the two metals propagate independently.¹⁵ There are no examples where the uranyl ion has been utilized in this polymerization, but the use of uranium(IV) compounds has been reported¹¹ which allows us to contrast the different oxidation states, and to compare with lanthanide aryloxides that are also known to be very active. It is worth emphasizing that we are not trying to design new, or more efficient, catalysts for this known polymerization reaction *per se*; rather, we are expanding upon our initial efforts to control the coordination geometry by the directing ability of the O=U=O fragment as the participation of 5f-orbitals in bonding enforces a *trans*-geometry which leaves the remainder of the coordination chemistry to occur in the equatorial plane. Using suitably sterically encumbered ligands to control the equatorial coordination sphere, mutually *cis*-ligand and solvent molecules can be coordinated. Therefore a catalytically competent geometry is an inherent property of the uranyl moiety, and is trivial to prepare, in stark contrast to transition metal catalysis where this geometry is enforced via ligand design. A strong U–O bond¹⁶ in the (pre)-catalyst is replaced by a U–O bond in the propagating polymer so that the contribution from enthalpy will be small and the polymerization will be entropically controlled. In this contribution, we explore the utility of **1** in the ring-opening polymerization of cyclic lactones (Figure 1).

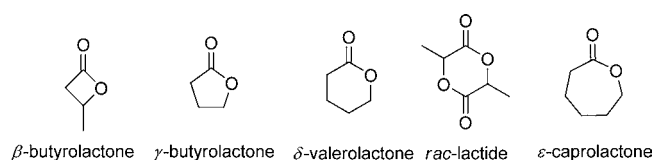


Figure 1. Monomers utilized in this study.

This allows us an ideal opportunity to systematically explore the steric constraints of the monomer and the electronics, specifically the ring strain as this varies with lactone ring size.

Despite the technical challenges of studying actinide compounds where relativistic and correlation effects are important to explicitly consider, there are a large number of computational studies on actinide metal containing com-

pounds.¹⁷ One of us has published extensively on a computational study of the ring-opening polymerization of lactones with lanthanide compounds,¹⁸ and herein we use computational chemistry to fully explore the mechanism of the ring-opening polymerization of δ -valerolactone and ϵ -caprolactone catalyzed by **1**. It is noteworthy that these calculations represent some of the largest to date especially considering that for mechanistic studies where we have located all transition states.

RESULTS AND DISCUSSION

Upon addition of ϵ -caprolactone to a solution of the uranyl aryloxide catalyst **1**, a color change to yellow was observed and a polymer precipitated out of solution over a period of time. The polymer was isolated and characterized by GPC, NMR spectroscopy and MALDI-ToF mass spectrometry. Figure 2 shows the % conversion of caprolactone with 1 mol % of catalyst and Table 1 collates the polymer characteristics for polymers obtained from **1** and, for comparison, selected f-block metal catalysts. The lanthanides are known to be superb catalysts for the ring-opening polymerization of ϵ -caprolactone, with high molecular weights and well controlled polydispersities obtained under mild conditions. While $[\text{Cp}^*_2\text{U}\text{Me}_2]$ shows excellent conversion to form high molecular weight polymers,^{11b} thorium 2-pyridylamidinates *cyclo*-oligomerize ϵ -caprolactone;^{11a} similar uranium(III) amidinate compounds have been reported to be substantially less active compared to analogous lanthanide compounds due to rapid oxidation to U(IV) by the monomer.¹⁹ **1** forms low molecular weight oligomers, which have a narrow polydispersity indicating well controlled oligomerization but a plot of % conversion vs. M_n does not give a straight line so this is not living. ^1H and $^{13}\text{C}\{^1\text{H}\}$ NMR spectroscopy and mass spectrometry (Figures S1 and S2, Supporting Information) shows no evidence of the expected end groups. This suggests that *cyclo*-oligomers are formed and we tentatively ascribe this to a backbiting termination step after a low number of insertions into the growing chain. The suggested mechanism for $[\text{Cp}^*_2\text{U}\text{Me}_2]$ or $[\text{U}(\text{NEt}_2)_3][\text{BPh}_4]$ is thought to be via a cationic mechanism with an observable end group in the polymer.

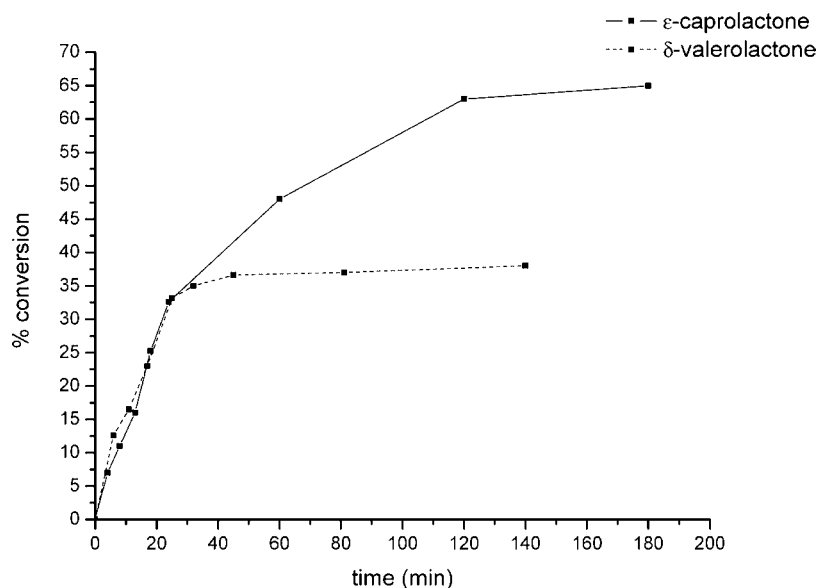


Figure 2. Ring-opening polymerization of ϵ -caprolactone and δ -valerolactone using **1** (25 °C in toluene).

Table 1. Polymerization of ϵ -Caprolactone (1:600 Catalyst Loading in Toluene)

catalyst	temp (°C)	time (h)	% conversion	M_n^a (gmol ⁻¹)	PDi	ref.
1	25	24	80	1500	1.20	this
1	100	8	74	1016	1.30	work
[Cp* ₂ UMe ₂]	25	24	61	30 000	1.09	11b
[Cp* ₂ UMe ₂]	110	0.25	99	50 000	1.49	11b
[U(NEt ₂) ₃][BPh ₄] ^b	25	0.25	100	57 000	1.24	11b
[(NCN) ₂ ThCl ₂] ^c	90	1		535	1.02	11a
				1300	1.05	
[(ArO) ₂ Sm(THF) ₃] ^d	25	0.03	100	153 000	1.43	20
[Cp* ₂ SmOEt(Et ₂ O)]	0	10	92	108 000	1.09	21

^aMark–Houwink correction applied.²² ^bIn THF. ^cNCN = 2-pyridylamidinate. ^d1:500 loading.

Further experiments were carried out to probe the polymerization, and these results are shown in Table 2. The

Table 2. Polymerization of ϵ -Caprolactone (1:600 Catalyst Loading in Toluene)

run	solvent	catalyst loading	time (h)	temp (°C)	% conversion	M_n^a	PDi
1	Toluene	1:600	5	25	86	1603	1.14
2	Toluene	1:300	5	25	48	1266	1.16
3	Toluene	1:100	5	25	79	1357	1.30
4	Toluene	1:100	0.5	100	55	1003	1.40
5	Toluene	1:100	5	100	76	1647	1.48
6	Toluene	1:100	24	100	89	2109	1.75
7	Toluene	1:300	24	25	80	1380	1.27
8	THF	1:300	24	25	48	2691	1.46
9	THF	1:600	5	70	47	2190	1.67
10	THF	1:300	5	70	49	1806	1.46
11	THF	1:100	5	70	48	1759	1.44
12	THF	1:600	5	25	44	2113	1.56
13	THF	1:300	5	25	43	2456	1.67
14	THF	1:100	5	25	45	2216	1.64

^aMark–Houwink correction applied.²²

molecular weights of the polymers are not dependent upon the catalyst loading as shown from runs 1–3 and 9–14. The molecular weight increases with time, but the molecular weight distribution also increases, presumably due to *trans*-esterification (runs 4–6). The solvent has an effect on the polymerization as in THF the polymers have higher molecular weights but also broader molecular weight distributions (runs 7–8); however, temperature does not have any obvious effect on the polymer characteristics. Also worthy of note is that in THF we have not observed conversion over 50%.

We have also examined the reactivity of **1** toward the ring-opening of other lactones (Figure 1), as the ring strain has been quantified for these.²³ β -Butyrolactone, δ -valerolactone and *rac*-lactide all contain strained rings and all have been polymerized by transition metal, lanthanide or main group metal compounds, although β -butyrolactone has been reported to be a significantly less reactive monomer,²⁴ and will allow us to benchmark the effectiveness of **1** compared to literature examples. γ -Butyrolactone does not have intrinsic ring strain and is not ring opened by metal-based catalysts.²⁵ Accordingly, the reactivity of **1** with these monomers was explored. We observe no polymerization of β -butyrolactone, which suggests our catalysts are not effective enough for the least reactive monomer in our survey. No polymerization was observed with γ -butyrolactone and in line with expectations.

Unexpectedly, *rac*-lactide did not polymerize, even under extended reflux in THF. This is in contrast to U(IV) metallocenes^{11b} and the diamido-ether actinide species [(NON)AnX₂] (NON = {(tBuNSiMe₂)₂O}²⁻; An = Th, U, X = CH₂SiMe₃, O^tBu, OⁱPr)²⁶ that polymerize this monomer to a high molecular weight polymer. δ -valerolactone did produce a polymer (M_n = 4689, PDi = 1.161), that did not have an end group by NMR or mass spectrometry. The percentage conversion is lower than for ϵ -caprolactone (Figure 2), as expected due to the lower ring strain, but the higher molecular weight suggests that larger *cyclo*-oligomers are formed with this monomer. This implies that the rate of termination is faster for ϵ -caprolactone than δ -valerolactone. It is interesting to note that the percentage conversion does not exceed 50%, and we are unsure why this is the case and further work is in progress. To the best of our knowledge, this is the first example of an actinide metal complex that ring opens this monomer, although lanthanide compounds are known with much higher molecular weights and faster polymerization kinetics.²⁷ The initial rates of polymerization of the lactones and epoxides are shown in Table 3. The greater rate for ring-opening of cyclohexene oxide is probably due to the release of the ring strain associated with the 6- and 3-membered rings.

Table 3. Initial Rates of Polymerization for Various Monomers Catalyzed by **1**

monomer	k_{obs} ($\times 10^{-2}$ min ⁻¹)
propylene oxide ^a	1.298 \pm 0.357
cyclohexene oxide ^a	2.708 \pm 0.573
δ -valerolactone	1.201 \pm 0.195
ϵ -caprolactone	1.074 \pm 0.102

^aFrom ref 9.

One reason for the lack of polymerization of *rac*-lactide may be due to the steric bulk of the monomer preventing coordination to the uranyl center. We have previously used ¹H EXSY spectroscopy to monitor monomer coordination and to determine the kinetic and thermodynamic parameters for the exchange of monomer and coordinated THF.⁹ When the addition of *rac*-lactide to the catalyst is examined, no exchange is observed confirming our steric argument. All other monomers do exchange with THF and a representative example of a ¹H EXSY spectrum is shown in Figure 3. As with our previous studies on epoxide polymerization, we have been unable to isolate coordination compounds with the monomer as oligomerization is observed to occur. By measuring the ¹H EXSY spectrum at different temperatures, the kinetic and thermodynamic parameters for the exchange

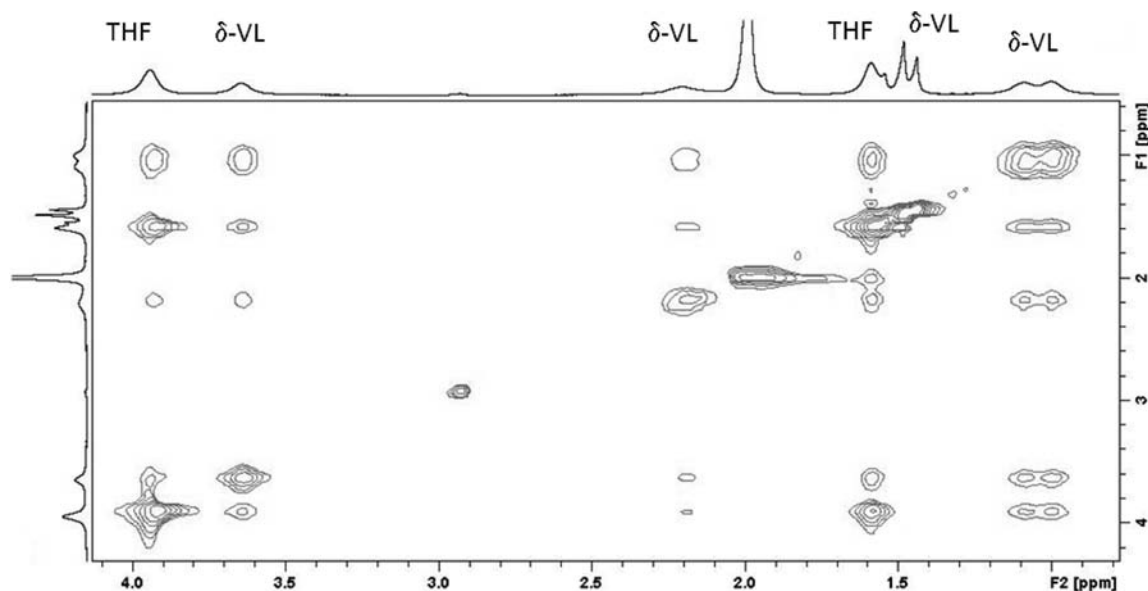


Figure 3. ^1H EXSY spectrum of **1** and <10 equiv of δ -valerolactone in C_6D_6 at 600 MHz ($T = 296$ K, $t_m = 1$ s).

Table 4. Kinetic and Thermodynamic Data for Exchange of Monomer and Coordinated THF in **1**

monomer	k (s^{-1} at 296 K)	E_{act} (kJ mol^{-1})	ΔH (kJ mol^{-1})	ΔS ($\text{J K}^{-1} \text{mol}^{-1}$)
propylene oxide	0.028 ± 0.002	-1.04 ± 0.03	0.71 ± 0.03	-235.06 ± 7
β -butyrolactone	0.031 ± 0.002	52.75 ± 19.5	-55.07 ± 19.4	-462.5 ± 133
γ -butyrolactone	0.022 ± 0.002	50.77 ± 7.2	-53.27 ± 1.6	-458.51 ± 173
δ -valerolactone	0.030 ± 0.003	-21.47 ± 8.8	16.81 ± 5.2	-223.56 ± 90
ϵ -caprolactone	0.012 ± 0.002	-19.49 ± 5.4	31.77 ± 8.8	-167.11 ± 96

process can be obtained;²⁸ Table 4 collates these parameters for the monomers in our study. The rates of exchange of monomer with coordinated THF are all similar, with the exception of ϵ -caprolactone. The thermodynamic parameters for those monomers that do polymerize are rather similar, and a negative entropy is indicative of an associative transition state. It is interesting to note that those that do not polymerize are thermodynamically distinct from those that do, and this is explored theoretically (*vide infra*). These results show that the rate determining step is not coordination of the monomer, but this is essential for polymerization to occur. It is also of note that the reaction of uranyl nitrate with either δ -valerolactone or ϵ -caprolactone affords stable 2:1 adducts, and the structure of $[\{\text{UO}_2(\eta^2\text{-NO}_3)(\eta^1\text{-caprolactone})\}_2(\mu_2\text{-O}_2)]$ is determined.²⁹ The nitrate ion is presumably insufficiently nucleophilic to initiate the ring-opening polymerization reaction.

As we observe *cyclo*-oligomers with no end group for both polymers, we can rule out a cationic mechanism as postulated for $[\text{Cp}^*_2\text{UMe}_2]$, and favor a coordination–insertion mechanism as postulated for $[(\text{NCN})_2\text{ThCl}_2]$ and for the ring-opening polymerization of propylene oxide. In order to explain the cyclic oligomers we postulate that intramolecular transesterification regenerates the U-OAr fragment to eventually deactivate, but not decompose, the catalyst. Support for this comes from the experiment where 100 equivalents of ϵ -caprolactone was added to a solution of **1** and stirred for 24 h. An aliquot was removed, quenched with MeOH and the molecular weight determined. A further 100 equivalents of ϵ -caprolactone was added to the catalyst solution and stirred for 24 h before quenching. NMR analysis showed little monomer remaining, while the M_n stayed approximately the same.

Further evidence comes from an examination of the polymer quenched using CD_3OD , and no signals were observed in the ^2H NMR spectrum.

We have carried out a kinetic analysis of the reaction and by standard techniques (Figure S5, Supporting Information) we have determined that the rate equation is first order in both monomer and catalyst. We postulate that the rate determining step is the nucleophilic attack of the electrophile upon the coordinated monomer in the initiation step as this has the greater steric bulk; in an intramolecular mechanism, the propagating step would be expected to release this steric pressure and hence of lower energy compared to the initiation. In order to comment upon the nature of the propagation (specifically inter- or intramolecular), we have used DOSY NMR spectroscopy, which gives the size of the molecules in solution.³⁰ The hydrodynamic radius of the catalyst is 4.82 \AA , which is in good agreement to that calculated from the X-ray structure (6.2 \AA). Upon addition of 5 equivalents of ϵ -caprolactone this increases to 9.80 \AA , which may suggest that the dominant species in solution is dimeric; the oligomers formed from ϵ -caprolactone have a larger hydrodynamic radius (Figure S6, Supporting Information).

To summarize the experimental findings, we have shown for the first time that uranyl aryloxides can ring open monomers with ring strain to form low molecular weight *cyclo*-oligomers. The kinetic data suggest that for the initiation step the mechanism is intramolecular (*cis*-migratory insertion), but DOSY NMR data tentatively suggest that an intermolecular propagation step may be in operation, consistent with the results from the ring-opening of epoxides. Therefore we have initiated a thorough computational examination of the

mechanism to gain further insight and confirm our experimentally postulated mechanism. First, the lack of polymerization of β - and γ -butyrolactone has been investigated theoretically. In both cases, the enthalpy for the displacement of a THF molecule by the monomer is found endothermic by 5.2 and 4.9 kcal.mol⁻¹ respectively, in good agreement with the experimental observation. Although the coordination is ensured by the carbonyl oxygen in all cases, the greater rigidity of the ring for the 4 and 5 member rings reduces the favorable C–H \cdots z interaction, that can be observed for the 6 and 7 member rings (Figure S7, Supporting Information). Thus, the coordination of the monomer is already difficult and it may explain the lack of reactivity of these monomers. The reaction mechanism for the two other monomers, namely δ -valerolactone and ϵ -caprolactone, will be investigated in detail. On the basis of our recent mechanistic study on the epoxide polymerization catalyzed by uranyl-aryloxide complexes,¹² the initiation step with the bulky (with respect to the propylene oxide monomer, PO) δ -valerolactone and ϵ -caprolactone monomers was only computed considering an intramolecular pathway (Figure 4). On the other hand, as the intermolecular

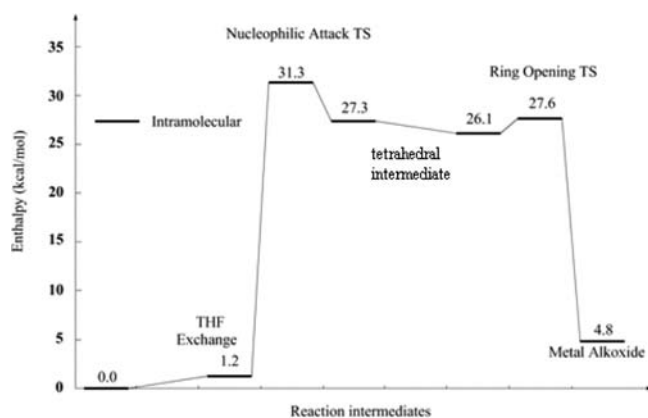
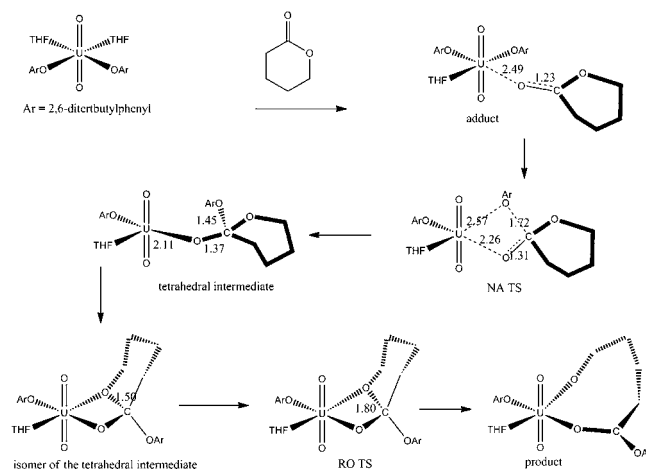


Figure 4. Computed reaction profile for the first insertion of δ -valerolactone.

pathway was found to be more favorable in the PO polymerization, both inter- and intramolecular routes were investigated in the propagation step (second insertion). The mechanism computed is “classical” of the ROP of cyclic lactones, involving a nucleophilic attack by the aryloxide leading to the formation of tetrahedral intermediate followed by the ring-opening. As it has already been studied theoretically by our group,^{18ij} it will not be commented on in detail and only the main energetic features will be discussed. A schematic representation of the stationary points is given in Scheme 2.

The reaction begins by the displacement of one THF molecule by a δ -valerolactone. This is predicted to be almost thermoneutral (+1.2 kcal mol⁻¹) in fair agreement with the experimental observation. Then, the system reaches the Nucleophilic Attack Transition state (NA TS), with an activation barrier of 31.3 kcal mol⁻¹ indicating a kinetically accessible, although quite energy demanding process. This barrier is mainly due to the intrinsic stability of the six-membered ring, making it hard to react with any nucleophile. This leads to the formation of a transient tetrahedral intermediate (at the carbon of the former ketone), which is highly unstable, and thus undergoes a ring-opening. The barrier for this ring-opening is very low (0.3 kcal mol⁻¹) from the

Scheme 2. Schematic Representation of the Initiation Step of the δ -Valerolactone ROP Catalyzed by a Monomeric Uranyl Complex^a



^aAll intermediates and transition states are depicted, along with important bond distances (Å).

intermediate, so that one can consider that it is a spontaneous process after the nucleophilic attack. The latter is thus the rate determining step of this first insertion.

To gain further insights on the reaction mechanism, the propagation step (second insertion) was computed (Figure 5).

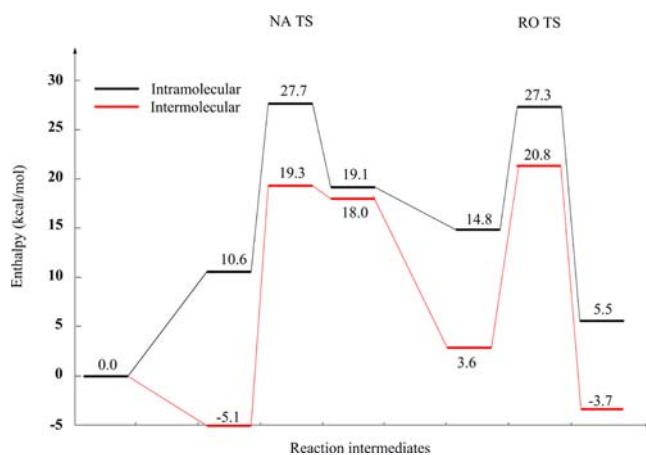
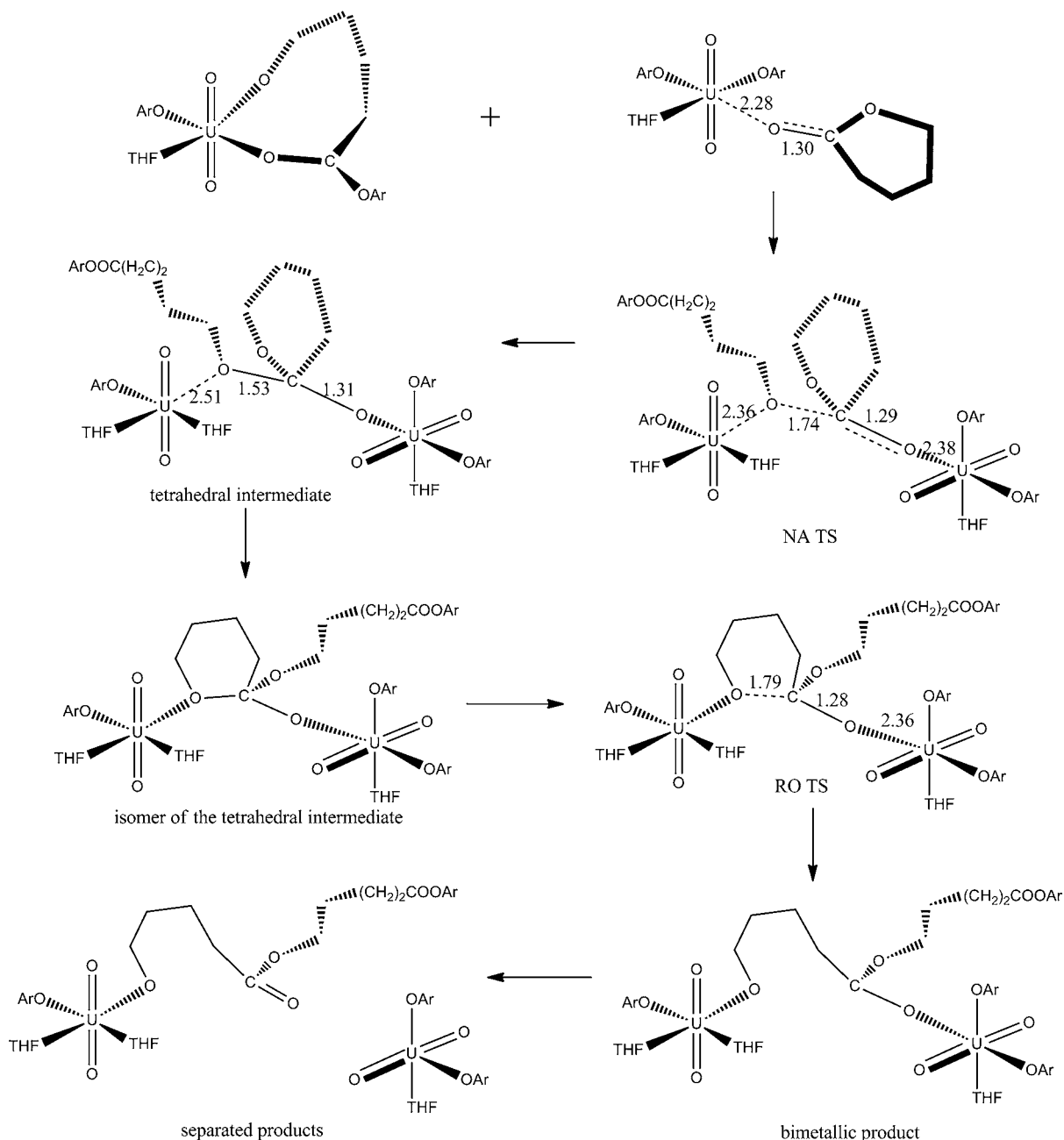


Figure 5. Computed reaction profile for the second insertion of δ -valerolactone.

The reaction mechanism for this second insertion is very similar to the one of the first insertion and the discussion will focus more on the difference between the intra- (Scheme 2) and intermolecular pathways (Scheme 3).

The intermolecular pathway is found to be favored thermodynamically and kinetically over the intramolecular one. This is somewhat similar to that reported in the case of PO polymerization. The main difference already occurs upon the coordination of the monomer to the metal center. Due to steric effects, the classical coordination of the δ -valerolactone *cis* to the alkoxide is disfavored making the intramolecular reaction pathway, which is to date the only one reported in the literature for cyclic lactone ROP, less favorable than the intermolecular one. Indeed, for the latter, the coordination to a second uranium center is even found to be exothermic by 5.1 kcal

Scheme 3. Schematic Representation of the Second Step of the δ -Valerolactone ROP Catalyzed by a Dimeric Uranyl Complex^a

^aAll intermediates and transition states are depicted, along with important bond distances (Å).

mol^{-1} ; a coordination energy in excellent agreement with the experimental observation ($3.9 \text{ kcal mol}^{-1}$). Then, the NA TS is reached (Figure 6), with a lower activation barrier for the intermolecular pathway ($24.6 \text{ vs } 27.7 \text{ kcal mol}^{-1}$). It is noteworthy that the second insertion is less energetically demanding than the first one, even when two uranyl complexes are involved. This is attributed to less steric hindrance around the metal center because the alkoxide exhibits a longer chain for second insertion than for the first one (aryloxide) pushing the aryl groups far from the uranium centers, and validating our experimental postulate. The NA TS also connects the tetrahedral intermediate (again at the carbon of the ketone), which is also found to be relatively unstable in both pathways. However, a stronger stabilization is found in the intramolecular

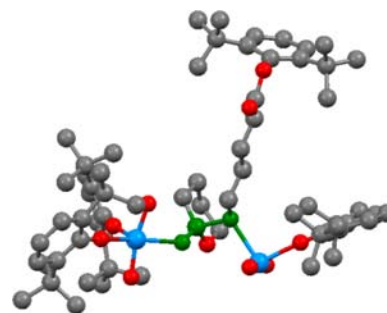


Figure 6. Geometry of the intermolecular nucleophilic attack TS. The green atoms are directly involved in the TS and the THF molecules have been omitted for clarity.

pathway than in the intermolecular one (roughly 10.0 kcal mol⁻¹ difference in stability). This increases the barrier for the ring-opening for the intramolecular pathway (12.5 kcal mol⁻¹), whereas the barrier is very low for the intermolecular one (roughly 3.0 kcal mol⁻¹), making the later more favorable. The origin of this enhanced stability is not known at this stage. The reaction energy is also more favorable when two metal centers are involved than with a single uranium catalyst. This is due to the formation of a very stable alkoxide dimer in the former case. This complex can be viewed as the resting state of the polymerization, and confirms our DOSY spectra. To summarize, the computed most favorable reaction pathway involves two uranium centers in an intermolecular reaction mechanism. To the best of our knowledge, such a mechanism has never been reported or even studied in the case of lactone ROP. However, due to the precision of the method, it is possible that both intra- and intermolecular pathways are operative.

In order to generalize this finding, the reaction of the uranyl catalyst with the popular ϵ -caprolactone has been studied. The reaction mechanism is very similar to the one computed for the δ -valerolactone, so that only the energetic features will be discussed.

The first insertion was also investigated only for the intramolecular pathway (Figure 7, Scheme S1, Supporting

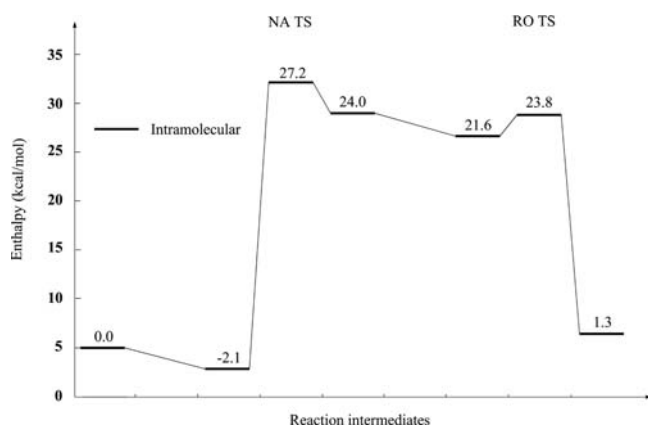


Figure 7. Computed reaction profile for the first insertion of ϵ -caprolactone.

Information). As expected and in agreement with the better polymerization ability of the ϵ -caprolactone, the barriers are lower for ϵ -caprolactone than the δ -valerolactone by roughly 4.0 kcal mol⁻¹. As for the δ -valerolactone case, both the intermolecular and the intramolecular pathway were investigated. Due to the size of the calculation, it has not been possible to fully characterize the ring-opening transition state for the intramolecular pathway (the frequency calculations failed even on supercomputer center) but it is expected to lead to a similar result as the δ -valerolactone, which is the lowest in energy (Figure 8, Scheme S2, Supporting Information). Interestingly, the coordination of ϵ -caprolactone with displacement of THF is found to be exothermic by 2.1 kcal mol⁻¹, indicating a favorable process, and in line with the experimental observation. As already found in the first insertion, the barriers are lower for ϵ -caprolactone than for δ -valerolactone but now by roughly 10.0 kcal mol⁻¹ (in the case of the monomer). Similarly to that calculated for δ -valerolactone, the intermolecular barriers are lower than the intramolecular ones, by

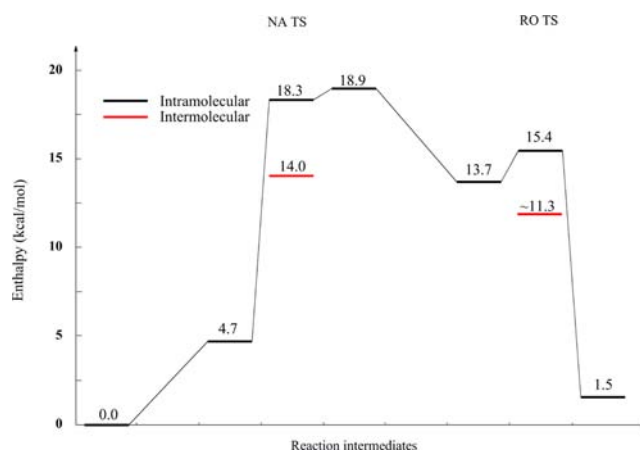


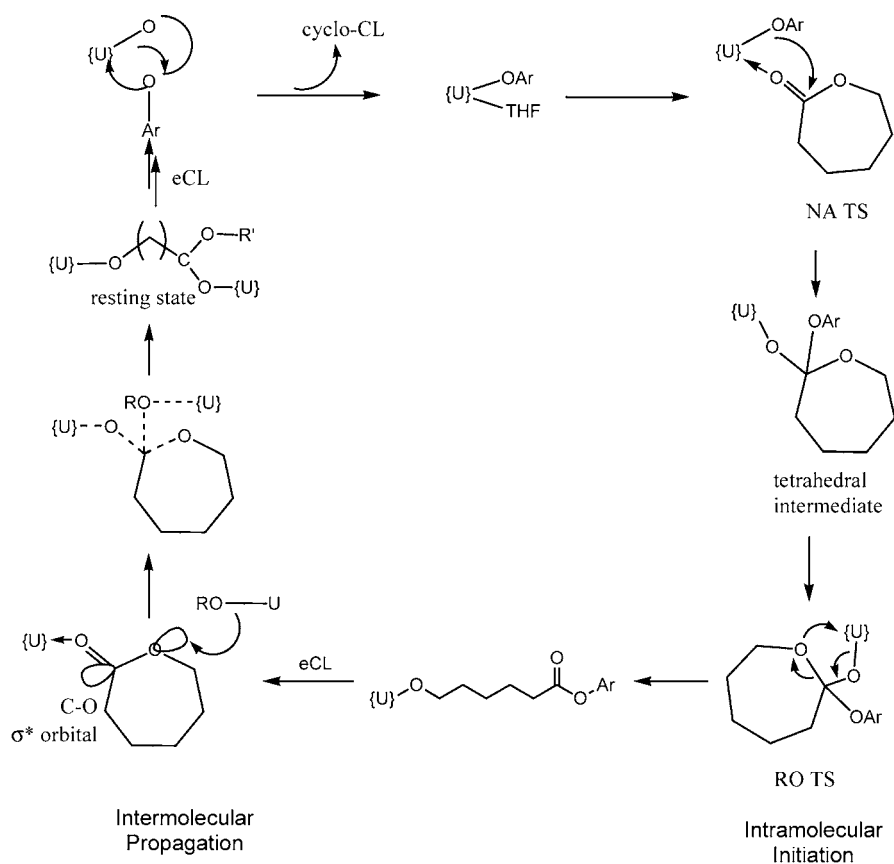
Figure 8. Computed reaction profile for the second insertion of ϵ -caprolactone.

roughly 4.0 kcal mol⁻¹. Thus, the intramolecular mechanism seems to be the favored pathway also in the case of the ϵ -caprolactone monomer.

On the basis of our spectroscopic and theoretical studies, we can propose a mechanism for the ring-opening polymerization of cyclic lactones by the uranyl aryloxide catalyst (Scheme 4). Initiation is an intramolecular process, which is the rate-determining step due to the steric constraints of the aryloxide ligand, but propagation may involve both *intra*- and *inter*-molecular pathways, with a binuclear resting state, that has been observed by DOSY NMR studies. We cannot calculate the hydrodynamic radius for the proposed resting state to compare with the DOSY experimental spectra, however the resting state for the corresponding δ -valerolactone structure, a calculated hydrodynamic radius of ca. 10 Å is similar to that found in the DOSY spectra. The intermolecular mechanism is quite unique, as to date only the ROP of epoxides invokes two metal centers, but this seems to be more general especially when bulky aryloxide ligands are involved. Also of note is that the change in enthalpy for the ring opened monomer compared to the catalyst is small, validating the initial postulate that uranyl ions can react with and turn over oxygen containing monomers providing a U–O bond is present in the catalyst.

CONCLUSION

In summary, based on our spectroscopic and theoretical investigations, we have proposed a mechanism of the ring-opening polymerization of lactones using a uranyl aryloxide. It has been shown to be an active catalyst in the ring-opening *cyclo*-oligomerization of ϵ -caprolactone and δ -valerolactone to form *cyclo*-oligomers. Interestingly, we see no evidence of the ring-opening of THF in any of our catalytic reactions; this reactivity has been noted in lower oxidation state uranium chemistry.³¹ The intermolecular (involving two uranyl catalysts, Scheme 4) reaction mechanism, based on our theoretical study, is proposed to be the most favorable but the intramolecular one may also operate at the same time. The energetic stability of the bimetallic alkoxide product, formed in the intermolecular mechanism, allows us to propose this complex to be the resting state of the polymerization rather than its monomeric analog. To the best of our knowledge, such a reaction mechanism has never been reported for the polymerization of lactones although is common for other monomers such as epoxides.

Scheme 4. Postulated Mechanism for Ring-opening Polymerization of ϵ -Caprolactone from Experimental and Computational Results

Thus, a number of mechanism studies of lactone ROP may have to be reinvestigated to consider intermolecular pathways.

EXPERIMENTAL SECTION

All manipulations were carried out using standard Schlenk and glovebox techniques under an atmosphere of high purity argon. Spectroscopic grade THF was distilled over potassium. ^1H NMR spectra were recorded on a Bruker AV400 spectrometer operating at 400.13 MHz and was referenced to the residual ^1H resonances of the solvent used. EXSY spectra were recorded using Bruker's NOESY pulse sequence; a number of mixing times were examined and 1 s was deemed optimal for all experiments. Kinetic data were extracted using the methodology described in ref 28 and are the average of three determinations. Details of the diffusion NMR can be found in the Supporting Information. Mass spectra were measured on a MALDI QTOF Premier MS system. GPC data was recorded on a Varian ProStar with a 350 RI detector using a PLgel 5 μm MIXED-D column and calibrated with EasiCal polystyrene standards; a Mark-Houwink correction was applied to the data.²² The complex $[\text{UO}_2(\text{OAr})_2(\text{THF})_2]^{32}$ was prepared by the literature procedure and all other reagents were obtained from commercial sources, dried over CaH_2 and distilled under Ar before use.

Polymerization Experiments. In a typical reaction, **1** was dissolved in PhMe or THF (10 cm^3) and placed in an oil bath set to the required temperature. After equilibrating for 15 min the monomer was added via syringe and the reaction vigorously stirred. After completion, MeOH/HCl (90:10) was added to quench the reaction and the polymer obtained as a solid or oil. This was washed with MeOH and dried under vacuum.

Determination of % conversion. During the course of the reaction, aliquots (ca. 1 cm^3) of the reaction mixture were removed, treated with one drop of MeOH and the ^1H NMR spectra were recorded. % conversion calculated from the relative integrals of the monomer (ϵ -

caprolactone: $\delta_{\text{H}} = 4.13$ ppm; δ -valerolactone: $\delta_{\text{H}} = 4.20$ ppm) and polymer (ϵ -caprolactone: $\delta_{\text{H}} = 3.68$ ppm; δ -valerolactone: $\delta_{\text{H}} = 4.37$ ppm).

COMPUTATIONAL DETAILS

In view of the good performance of density functional theory (DFT), we were prompted to perform DFT calculations at the B3PW91 level of theory on all stationary points of the potential energy surfaces (PES) we studied using the GAUSSIAN09 program suite.³³ The equilibrium and transition structures were fully optimized at the Becke's 3-parameter hybrid functional³⁴ combined with the nonlocal correlation functional provided by Perdew/Wang.³⁵ RECP (augmented by a f polarization function, $\alpha = 1.0$) adapted to the oxidation state +VI was used for the reactions.³⁶ The correctness of the latter is well documented in previous publications from our group.³⁷ For the rest of nonmetal atoms the 6-31G(d,p) basis set was used.³⁸ In all computations, no constraints were imposed on the geometry. Full geometry optimization was performed for each structure using Schlegel's analytical gradient method³⁹ and the attainment of the energy minimum was verified by calculating the vibrational frequencies that result in absence of imaginary eigenvalues. All stationary points have been identified for minimum (number of imaginary frequencies $N_{\text{imag}} = 0$) or transition states ($N_{\text{imag}} = 1$). The vibrational modes and the corresponding frequencies are based on a harmonic force field. This was achieved with the SCF convergence on the density matrix of at least 10^{-9} and the rms force less than 10^{-4} au. All bond lengths and bond angles were optimized to better than 0.001 Å and 0.1° , respectively. Gibbs free energies were obtained at $T = 298.15$ K within the harmonic approximation. Intrinsic Reaction Paths (IRPs)⁴⁰ were traced from the various transition structures to ensure that no further intermediates exist.

■ ASSOCIATED CONTENT

■ Supporting Information

Further spectroscopic and computational data. This material is available free of charge via the Internet at <http://pubs.acs.org>.

■ AUTHOR INFORMATION

Corresponding Author

*E-mail: bakerrj@tcd.ie (R.J.B.), laurent.maron@irsamc.upstlse.fr (L.M.).

Author Contributions

The manuscript was written through contributions of all authors. All authors have given approval to the final version of the manuscript.

Notes

The authors declare no competing financial interest.

■ ACKNOWLEDGMENTS

We thank IRCSET for funding this work through the EMBARK initiative (A.W. and R.J.B.) and the French Ministry of Research and Higher Education, INSA and UPS are thanked for financial support. L.M. is grateful to the Institut Universitaire de France. CalMip (CNRS, Toulouse, France) and CINES (CNRS, Montpellier, France) are acknowledged for calculation facilities. J.F. thanks the financial support from the Chinese Scholarship Council (CSC) and the Scholarship Council of Lanzhou University.

■ REFERENCES

- (1) (a) Mougél, V.; Camp, C.; Pécaut, J.; Copéret, C.; Maron, L.; Kefalidis, C. E.; Mazzanti, M. *Angew. Chem., Int. Ed.* **2012**, *51*, 12280–12284. (b) Schmidt, A.-C.; Nizovtsev, A. V.; Scheurer, A.; Heinemann, F. W.; Meyer, K. *Chem. Commun.* **2012**, *48*, 8634–8636. (c) King, D. M.; Tuna, F.; McInnes, E. J. L.; McMaster, J.; Lewis, W.; Blake, A. J.; Liddle, S. T. *Science* **2012**, *337*, 717–720. (d) Gardner, B. M.; Stewart, J. C.; Davis, A. L.; McMaster, J.; Lewis, W.; Blake, A. J.; Liddle, S. T. *Proc. Natl. Acad. Sci. U.S.A.* **2012**, *109*, 9265–9270. (e) Lamb, O. P.; Meyer, K. *Polyhedron* **2012**, *32*, 1–9. (f) Lam, O. P.; Heinemann, F. W.; Meyer, K. *Chem. Sci.* **2011**, *2*, 1538–1547. (g) Arnold, P. L. *Chem. Commun.* **2011**, *47*, 9005–9010. (h) Summerscales, O. T.; Cloke, F. G. N. *Struct. Bonding (Berlin)* **2008**, *127*, 87–117. (i) Lam, O. P.; Anthon, C.; Meyer, K. *Dalton Trans.* **2009**, 9677–9691.
- (2) (a) Jones, M. B.; Gaunt, A. J. *Chem. Rev.* **2013**, *113*, 1137–1198. (b) Baker, R. J. *Coord. Chem. Rev.* **2012**, *256*, 2843–2871. (c) Hayton, T. W. *Dalton Trans.* **2010**, *39*, 1145–1158. (d) Liddle, S. T.; Mills, D. P. *Dalton Trans.* **2009**, 5592–5605. (e) Liddle, S. T. *Proc. R. Soc. A* **2009**, *465*, 1673–1700. (f) Castro-Rodríguez, I.; Meyer, K. *Chem. Commun.* **2006**, 1353–1368. (g) Ephritikhine, M. *Dalton Trans.* **2006**, 2501–2516.
- (3) Baker, R. J. *Chem.—Eur. J.* **2012**, *18*, 16258–16271.
- (4) Tournoux, J.-C.; Berthet, J.-C.; Cantat, T.; Thuéry, P.; Mézailles, N.; Ephritikhine, M. *J. Am. Chem. Soc.* **2011**, *133*, 6162–6165.
- (5) Mills, D. P.; Cooper, O. J.; Tuna, F.; McInnes, E. J. L.; Davies, E. S.; McMaster, J.; Moro, F.; Lewis, W.; Blake, A. J.; Liddle, S. T. *J. Am. Chem. Soc.* **2012**, *134*, 10047–10054.
- (6) (a) Graves, C. R.; Kiplinger, J. L. *Chem. Commun.* **2009**, 3831–3853. (b) Arnold, P. L.; Love, J. B.; Patel, D. *Coord. Chem. Rev.* **2009**, *253*, 1973–1978.
- (7) Mougél, V.; Chatelain, L.; Pécaut, J.; Caciuffo, R.; Colineau, E.; Griveau, J.-C.; Mazzanti, M. *Nat. Chem.* **2012**, *4*, 1011–1017.
- (8) Nyman, M.; Burns, P. C. *Chem. Soc. Rev.* **2012**, *41*, 7354–7367.
- (9) Baker, R. J.; Walshe, A. *Chem. Commun.* **2012**, *48*, 985–987.
- (10) Lin, Z.; Marks, T. J. *J. Am. Chem. Soc.* **1987**, *109*, 7979–7985.
- (11) (a) Rabinovich, E.; Aharonovich, S.; Botoshansky, M.; Eisen, M. S. *Dalton Trans.* **2010**, *39*, 6667–6676. (b) Barnea, E.; Moradove, D.;

Berthet, J.-C.; Ephritikhine, M.; Eisen, M. S. *Organometallics* **2006**, *25*, 320–322.

(12) Fang, J.; Walshe, A.; Maron, L.; Baker, R. J. *Inorg. Chem.* **2012**, *51*, 9132–9140.

(13) For recent reviews, see: (a) Stanford, M. J.; Dove, A. P. *Chem. Soc. Rev.* **2010**, *39*, 486–494. (b) Labet, M.; Thielemans, W. *Chem. Soc. Rev.* **2009**, *38*, 3484–3504. (c) Wheaton, C. A.; Hayes, P. G.; Ireland, B. J. *Dalton Trans.* **2009**, 4832–4846. (d) Kamber, N. E.; Jeong, W.; Waymouth, R. M.; Pratt, R. C.; Lohmeijer, B. G. G.; Hedrick, J. L. *Chem. Rev.* **2007**, *107*, 5813–5840. (e) Chen, C.-T.; Lin, C.-C. *Coord. Chem. Rev.* **2006**, *250*, 602–626.

(14) Representative examples: (a) Douglas, A. F.; Patrick, P. O.; Mehrkhodavandi, P. *Angew. Chem., Int. Ed.* **2008**, *47*, 2290–2293. (b) Tang, H.-Y.; Chen, H.-Y.; Huang, J.-Y.; Lin, C.-C. *Macromolecules* **2007**, *40*, 8855–8860. (c) Williams, C. K.; Breyfogle, L. E.; Choi, S. K.; Nam, W.; Voung, V. G., Jr.; Hillmyer, M. A.; Tolman, W. B. *J. Am. Chem. Soc.* **2003**, *125*, 11350–11359.

(15) Representative examples: (a) Shen, M.-Y.; Peng, Y.-L.; Hung, W.-C.; Lin, C.-C. *Dalton Trans.* **2009**, 9906–9913. (b) Gao, A.-H.; Yao, W.; Mu, Y.; Gao, W.; Sun, M.-T.; Su, Q. *Polyhedron* **2009**, *28*, 2605–2610.

(16) The bond disruption energy of a U(IV)–O bond is 307 ± 13 kJ mol⁻¹: Leala, J. P.; Marques, N.; Takats, J. *J. Organomet. Chem.* **2001**, *632*, 209–214.

(17) For recent reviews, see: (a) Dolg, M.; Cao, X. In *Encyclopedia of Inorganic Chemistry*, 2nd ed.; John Wiley & Sons, Ltd: New York, 2006. (b) Gagliardi, L.; Roos, B. O. *Chem. Soc. Rev.* **2007**, *36*, 893–903. (c) Kaltsoyannis, N. *Chem. Soc. Rev.* **2003**, *32*, 9–16. (d) Schreckenbach, G.; Shamov, G. A. *Acc. Chem. Res.* **2010**, *43*, 19–29. (e) Wang, D.; van Gunsteren, W. F.; Chai, Z. *Chem. Soc. Rev.* **2012**, *41*, 5836–5865.

(18) (a) Momin, A.; Bonnet, F.; Visseaux, M.; Maron, L.; Takats, J.; Ferguson, M. J.; Le Goff, X.-F.; Nief, F. *Chem. Commun.* **2011**, *47*, 12203–12205. (b) del Rosal, I.; Poteau, R.; Maron, L. *Dalton Trans.* **2011**, *40*, 11211–11227. (c) del Rosal, I.; Poteau, R.; Maron, L. *Dalton Trans.* **2011**, *40*, 11228–11240. (d) Iftner, C.; Bonnet, F.; Nief, F.; Visseaux, M.; Maron, L. *Organometallics* **2011**, *30*, 4482–4485. (e) Guillaume, S. M.; Brignou, P.; Susperregui, N.; Maron, L.; Kuzdrowska, M.; Roesky, P. W. *Polym. Chem.* **2011**, *2*, 1728–1736. (f) Susperregui, N.; Kramer, M. U.; Okuda, J.; Maron, L. *Organometallics* **2011**, *30*, 1326–1333. (g) Perrin, L.; Bonnet, F.; Chenal, T.; Visseaux, M.; Maron, L. *Chem.—Eur. J.* **2010**, *16*, 11376–11385. (h) Dyer, H. E.; Huijser, S.; Susperregui, N.; Bonnet, F.; Schwarz, A. D.; Duchateau, R.; Maron, L.; Mountford, P. *Organometallics* **2010**, *29*, 3602–3621. (i) Jenter, J.; Roesky, P. W.; Ajellal, N.; Guillaume, S. M.; Susperregui, N.; Maron, L. *Chem.—Eur. J.* **2010**, *16*, 4629–4638. (j) Barros, N.; Mountford, P.; Guillaume, S. M.; Maron, L. *Chem.—Eur. J.* **2008**, *14*, 5507–5518.

(19) Villiers, C.; Thuéry, P.; Ephritikhine, M. *Eur. J. Inorg. Chem.* **2004**, 4624–4632.

(20) Nishiura, M.; Hou, Z.; Koizumi, T.-A.; Imamoto, T.; Wakatsuki, Y. *Macromolecules* **1999**, *32*, 8245–8251.

(21) Yamashita, M.; Takemoto, Y.; Ihara, E.; Yasuda, H. *Macromolecules* **1996**, *29*, 1798–1806.

(22) (a) Kowalski, A.; Duda, A.; Penczek, S. *Macromolecules* **1998**, *31*, 2114–2122. (b) Duda, A.; Florjanczyk, Z.; Hofman, A.; Slomkowski, S.; Penczek, S. *Macromolecules* **1990**, *23*, 1640–1646.

(23) (a) Alemán, C.; Betran, O.; Casanovas, J.; Houk, K. N.; Hall, H. K., Jr. *J. Org. Chem.* **2009**, *74*, 6237–6244. (b) Houk, K. N.; Jabbari, A. H.; Hall, H. K., Jr.; Alemán, C. *J. Org. Chem.* **2008**, *73*, 2674–2678.

(24) For recent references, see: (a) Carpentier, J.-F. *Macromol. Rapid Commun.* **2010**, *31*, 1696–1705. (b) Thomas, C. M. *Chem. Soc. Rev.* **2010**, *39*, 165–173. (c) Lutz, J.-F. *Nat. Chem.* **2010**, *2*, 84–85. (c) Amgoune, A.; Thomas, C. M.; Ilinca, S.; Roisnel, T.; Carpentier, J.-F. *Angew. Chem., Int. Ed.* **2006**, *45*, 2782–2784.

(25) Moore, T.; Adhikaria, R.; Gunatillake, P. *Biomaterials* **2005**, *26*, 3771–3782.

(26) Hayes, C. E.; Sarazin, Y.; Katz, M. J.; Carpentier, J.-F.; Leznoff, D. B. *Organometallics* **2013**, *32*, 1183–1192.

(27) Selected references: (a) Nakayama, Y.; Sasaki, K.; Watanabe, N.; Cai, Z.; Shiono, T. *Polymer* **2009**, *50*, 4788–4793. (b) Dietrich, H. M.; Törnroos, K. W.; Anwander, R. *J. Am. Chem. Soc.* **2006**, *128*, 9298–9299. (c) Nishiura, M.; Hou, Z.; Koizumi, T.; Imamoto, T.; Wakatsuki, Y. *Macromolecules* **1999**, *32*, 8245–8251. (d) Yamashita, M.; Takemoto, Y.; Ihara, E.; Yasuda, H. *Macromolecules* **1996**, *29*, 1798–1806.

(28) Günther, H. *NMR spectroscopy: basic principles, concepts, and applications in chemistry*, 2nd ed.; Wiley: Chichester, 1995.

(29) de Aquino, A. R.; Isolani, P. C.; Zukerman-Schpector, J.; Zinner, L. B.; Vicentini, G. *J. Alloys Compd.* **2001**, *323–324*, 18–21.

(30) Selected reviews: (a) Macchioni, A.; Ciancaleoni, G.; Zuccaccia, C.; Zuccaccia, D. *Chem. Soc. Rev.* **2008**, *37*, 479–489. (b) Pregosin, P. S.; Kumar, P. G. A.; Fernández, I. *Chem. Rev.* **2005**, *105*, 2977–2998.

(31) (a) Takase, M. K.; Ziller, J. W.; Evans, W. J. *Chem.—Eur. J.* **2011**, *17*, 4871–4878. (b) Evans, W. J.; Kozimor, S. A.; Ziller, J. W. *J. Am. Chem. Soc.* **2003**, *125*, 14264–14265. (c) Boisson, C.; Berthet, J.-C.; Lance, M.; Nierlich, M.; Ephritikhine, M. *Chem. Commun.* **1996**, 2129–2130. (d) Avens, L. R.; Barnhart, D. M.; Burns, C. J.; McKee, S. D. *Inorg. Chem.* **1996**, *35*, 537–539. (e) Campello, M. P. C.; Domingos, A.; Santos, I. *J. Organomet. Chem.* **1994**, *484*, 37–46. (f) Collin, J.; Pires de Matos, A.; Santos, I. *J. Organomet. Chem.* **1993**, *463*, 103–107.

(32) Wilkerson, M. P.; Burns, C. J.; Morris, D. E.; Paine, R. T.; Scott, B. L. *Inorg. Chem.* **2002**, *41*, 3110–3120.

(33) Frisch, M. J.; Trucks, G. W.; Schlegel, H. B.; Scuseria, G. E.; Robb, M. A.; Cheeseman, J. R.; Scalmani, G.; Barone, V.; Mennucci, B.; Petersson, G. A.; Nakatsuji, H.; Caricato, M.; Li, X.; Hratchian, H. P.; Izmaylov, A. F.; Bloino, J.; Zheng, G.; Sonnenberg, J. L.; Hada, M.; Ehara, M.; Toyota, K.; Fukuda, R.; Hasegawa, J.; Ishida, M.; Nakajima, T.; Honda, Y.; Kitao, O.; Nakai, H.; Vreven, T.; Montgomery, J. A., Jr.; Peralta, J. E.; Ogliaro, F.; Bearpark, M.; Heyd, J. J.; Brothers, E.; Kudin, K. N.; Staroverov, V. N.; Kobayashi, R.; Normand, J.; Raghavachari, K.; Rendell, A.; Burant, J. C.; Iyengar, S. S.; Tomasi, J.; Cossi, M.; Rega, N.; Millam, J. M.; Klene, M.; Knox, J. E.; Cross, J. B.; Bakken, V.; Adamo, C.; Jaramillo, J.; Gomperts, R.; Stratmann, R. E.; Yazyev, O.; Austin, A. J.; Cammi, R.; Pomelli, C.; Ochterski, J. W.; Martin, R. L.; Morokuma, K.; Zakrzewski, V. G.; Voth, G. A.; Salvador, P.; Dannenberg, J. J.; Dapprich, S.; Daniels, A. D.; Farkas, O.; Foresman, J. B.; Ortiz, J. V.; Cioslowski, J.; Fox, D. J. *Gaussian 09*, Revision A.02; Gaussian, Inc.: Wallingford, CT, 2009.

(34) Becke, A. D. *J. Chem. Phys.* **1993**, *98*, 5648–5652.

(35) Perdew, J. P.; Wang, Y. *Phys. Rev. B* **1992**, *45*, 13244–13249.

(36) Moritz, A.; Cao, X. Y.; Dolg, M. *Theor. Chem. Acc.* **2007**, *118*, 845–854.

(37) (a) Castro, L.; Yahia, A.; Maron, L. *ChemPhysChem* **2010**, *11*, 990–994. (b) Castro, L.; Yahia, A.; Maron, L. *Dalton Trans.* **2010**, *39*, 6682–6692.

(38) (a) Ditchfield, R.; Hehre, W. J.; Pople, J. A. *J. Chem. Phys.* **1971**, *54*, 724–728. (b) Hehre, W. J.; Ditchfield, R.; Pople, J. A. *J. Chem. Phys.* **1972**, *56*, 2257–2261. (c) Hariharan, P. C.; Pople, J. A. *Theor. Chim. Acta* **1973**, *28*, 213–223.

(39) Schlegel, H. B. *J. Comput. Chem.* **1982**, *3*, 214–218.

(40) (a) Gonzalez, C.; Schlegel, H. B. *J. Chem. Phys.* **1989**, *90*, 2154–2161. (b) Gonzalez, C.; Schlegel, H. B. *J. Phys. Chem.* **1990**, *94*, 5523–5527.